MOLECULAR IMAGING AND BIOLOGY

Mol Imaging Biol (2019) 21:286–296
DOI: 10.1007/s11307-018-1234-7

Published Online: 18 June 2018

RESEARCH ARTICLE

Noninvasive PET Imaging of a Ga-68-Radiolabeled RRL-Derived Peptide in Hepatocarcinoma Murine Models

Yan Huo, Lei Kang, Xiaoxi Pang, Haoyuan Shen, Ping Yan, Chunli Zhang, Xuhe Liao, Xueqi Chen, Rongfu Wang

Department of Nuclear Medicine, Peking University First Hospital, No. 8 St. Xishiku, Beijing, 100034, China

Abstract

Purpose: Tc-99m- and I-131-labeled arginine-arginine-leucine (RRL) peptides have shown the feasibility of tumor imaging in our previous studies. However, there have been no reports using RRL peptide for positron emission tomography (PET) imaging. In this study, RRL was radiolabeled with Ga-68 under optimized reaction conditions to develop a better specific and effective tumor imaging agent.

Procedures: RRL was synthesized and conjugated to a bifunctional chelating agent (DOTA-NHS), then radiolabeled with Ga-68. Labeling yield was optimized by varying pH, temperature, and reaction time and the stability was evaluated in human fresh serum. Cellular uptakes of [^{68}Ga]DOTA-RRL and FITC-conjugated RRL in HepG2 cells were evaluated using a gamma counter, confocal microscopy, and flow cytometry. PET images and biodistribution were performed in HepG2 tumor-bearing mice after injection of [^{68}Ga]DOTA-RRL or [^{68}Ga]$GaCl_3$ at different time points. Further, blocking study was investigated using cold RRL.

Results: The labeling yield of [^{68}Ga]DOTA-RRL was 80.6 ± 3.9 % with a pH of 3.5–4.5 at 100 °C for 15 min. The cellular uptake of [^{68}Ga]DOTA-RRL in HepG2 cells was significantly higher than that of [^{68}Ga]$GaCl_3$ ($P < 0.05$). Moreover, the high fluorescent affinity of FITC-conjugated RRL in HepG2 cells was shown using confocal microscopy and flow cytometry. After injection of [^{68}Ga]DOTA-RRL in HepG2 tumor-bearing mice, tumor regions exhibited high radioactive accumulation over 120 min and the highest uptake at 30 min. After blocked with cold RRL, HepG2 tumors could not be visualized. [^{68}Ga]$GaCl_3$ was unable to show tumor images at any time point. The biodistribution results confirmed the PET imaging and blocking results.

Conclusions: Our study successfully prepared [^{68}Ga]DOTA-RRL with a high labeling yield under the optimized reaction conditions and demonstrated its potential role as a PET imaging agent for tumor-targeted diagnosis.

Key words: Arginine-arginine-leucine (RRL), Peptide, Molecular imaging, Gallium-68 (^{68}Ga), Hepatocarcinoma

Introduction

Small peptides have distinct advantages in cancer diagnosis and therapy. The cost to synthesize them is relatively low; they are less likely to induce an immunogenic response and they have rapid blood clearance [1]. Tripeptide, arginine-

Yan Huo and Lei Kang contributed equally to this work.

Electronic supplementary material The online version of this article (https://doi.org/10.1007/s11307-018-1234-7) contains supplementary material, which is available to authorized users.

Correspondence to: Rongfu Wang; *e-mail:* rongfu_wang2003@163.com

arginine-leucine (RRL), was initially identified using an *in vitro* bacterial peptide display library (FLiTrx) against tumor-derived endothelial cell derived from SCC-VII murine squamous cell carcinomas [2]; therefore, it was found to bind tumor endothelial cells specifically. Some other tumor angiogenesis-targeted peptides such as asparagines-glycine-arginine (NGR) and arginine-glycine-aspartate (RGD) have been widely studied [3]. In the comparison, RRL peptide was not only considered as a tumor vessel endothelial cell-targeted peptide [4, 5] but also was shown to have a strong binding affinity to cancer parenchyma cells [6, 7], which might provide a better candidate for tumor targeting.

Based on the binding properties of RRL to tumor cells, we developed a nuclear medicine agent by radioiodinating RRL for *in vivo* prostate cancer imaging [8]. We have also developed several Tc-99m- and I-131-radiolabeled RRL peptides for *in vivo* tumor and neovascular imaging [9–12]. However, these SPECT-based studies had limited sensitivity and resolution for *in vivo* imaging [13]. For this purpose, using positron emission tomography (PET) imaging to visualize RRL can overcome these limitations because of its high sensitivity in the real-time detection of molecular events [14].

Gallium-68 is an ideal radionuclide for diagnostic imaging due to a short half-life ($t_{1/2} = 68$ min), a suitable time interval, and low radiation dosimetry for imaging [15, 16]. In comparison to some other positron-emitted radionuclides (F-18, Cu-64, Zr-89), Ga-68 is readily commercially available and easily produced by Ge-68/Ga-68 generator, avoiding the need for a cyclotron [15]. For Ga-68 labeling, a variety of bifunctional chelators (BFC) can be effectively used due to their high hydrophilicity and *in vivo* stability. As a common commercial chelator, 1,4,7,10-tetraazacyclododecane-1,4,7,10-tetraacetic acid (DOTA) can be used for Ga-68 labeling fast and efficiently [16]. As a result of these advantages, there has been an increase in the interest in the application for Ga-68-labeled peptides.

In this study, we prepared a novel Ga-68-labeled RRL peptide *via* the conjugation with DOTA for a potential PET tumor imaging agent. The radiolabeling of [^{68}Ga]DOTA-RRL was optimized by varying pH, temperature, and reaction time. Cellular uptake of [^{68}Ga]DOTA-RRL and cellular binding of fluorescent RRL in human hepatocarcinoma (HepG2) cell line were evaluated. The *in vivo* PET imaging and biodistribution of [^{68}Ga]DOTA-RRL was investigated in HepG2 tumor-bearing mice. Finally, the specificity of RRL was evaluated *via* inhibition with the cold RRL peptide.

Materials and Methods

Cell Culture and Tumor Model

The human hepatocarcinoma cancer HepG2 and human amniotic epithelial cell (HAEC) cell lines were obtained from the American Type Culture Collection and cultured according to the supplier's instructions. All animal experiments were approved by Peking University Animal Studies Committee, according to the guidelines for the Care and Use of Research Animals (Peking University, China) (Approval ID J201138). HepG2 tumor-bearing models were built by subcutaneous injection of 1×10^7 HepG2 cells in nu/nu nude mice. When the diameter of tumors reached 1 cm, mice were used for PET imaging and biodistribution studies.

Peptide Design and Synthesis

RRL peptide was designed and modified according to previous studies [10, 11]. Briefly, Cys-Gly-Gly peptides were linked to each side of RRL to form and maintain a cyclic structure *via* a disulfide bond [17]. The amidated cysteine at the C-terminal and cyclic structure was used to protect the peptides from rapid biodegradation [18]. 4-Abz was linked to the terminal to reduce the impact of steric hindrance on labeling efficiency and to stabilize the labeled compound. The final sequence of RRL was NH_2-Gly-4-Abz-Cys-Gly-Gly-Arg-Arg-Leu-Gly-Gly-Cys. RRL peptides were chemically modified and synthesized using the chemical solid phase method from GL Biochem Ltd. (Shanghai, China). Fluorescent isothiocyanate (FITC)-conjugated RRL was also synthesized and bought from GL Biochem Ltd. (Shanghai, China) for cellular binding assay.

DOTA Conjugation and Radiolabeling Optimization

DOTA-NHS-ester was purchased from Macrocyclics Co. (USA) to chelate Ga^{3+} ions [19]. DOTA-conjugated RRL was prepared according to the previous method [20]. Briefly, RRL peptide was dissolved in 0.1 M PBS and mixed with DOTA in DMF solution at the molecular ratio of RRL to DOTA of 1:10. The pH of the mixture was to 8.5–9.0 using carbonate buffer. The mixture was then shocked gently at room temperature (RT) for 2 h. Excess chelator was removed by size exclusion chromatography using a PD-10 column with 0.1 M PBS buffer. Fractions of 1 ml were collected from the column and tested using high-performance liquid chromatography (HPLC). The purified product was lyophilized and stored at − 20 °C.

Ga-68 was produced using a Ge-68/Ga-68 generator (Isotope Technologies Garching GmbH, Germany). In accordance with the protocol from the manufacturer, Ga-68 was eluted with 5 ml of 0.1 N hydrochloric acid. For labeling, 1 ml (185 MBq) of [^{68}Ga]$GaCl_3$ was added to a clean tube in which varying amounts of 1.25 N sodium acetate buffer were added to study the influence of pH (< 3, 3.5–4, > 5) in combination with 1 mg/ml of peptide-chelator PBS solution (50 μg of peptides included). To optimize the radiolabeling efficiency with respect to the temperature and reaction time, the mixture was heated at different temperatures including 37, 60, and 100 °C for 10, 15, and 20 min,

respectively. Each radiolabeling reaction was evaluated by instant thin-layer chromatography (ITLC) with the mobile phase of a methanol/acetic acid (volume ratio of 9:1). The radiolabeled product was evaluated using HPLC.

Polyacrylamide Gel Electrophoresis (PAGE) Assay

To assess the stability of DOTA-RRL at different radiolabeling reaction temperatures, DOTA-RRL (30 μg) was incubated at RT, 60 and 100 °C for 20 min. DOTA-RRL was loaded and analyzed by polyacrylamide gel electrophoresis assay at 120 V for 20 min. Proteins gel was stained with coomassie dye G-250 for 1 h and washed with water for 40 min before evaluation.

Stability Evaluation

3.7 MBq of [^{68}Ga]DOTA-RRL was incubated in human fresh serum or saline at 37 °C at the concentration of 20 μg/ml for 1, 2, and 4 h. At the different time points, the radiochemical purity was measured by instant thin-layer chromatography silica gel (ITLC-SG) using a methanol and ammonium acetate solvent (volume ratio of 1:1).

Cellular Radioactivity Uptake

In vitro cellular uptake was performed in 24-well plates with 1×10^5 HepG2 cells per well ($n = 3$). [^{68}Ga]DOTA-RRL or [^{68}Ga]$GaCl_3$ (74 kBq/well) was incubated at 37 °C for 0.5, 1, and 2 h. After the medium was removed, cells were washed with PBS for three times. Cells were then lysed using 0.5 M sodium hydroxide and 1 % sodium dodecyl sulfate and washed for three times. The cellular uptake ratio was calculated by dividing the radio counts of lysis to the sum of those of medium and lysis.

Confocal Microscopy

HepG2 and HAEC cells were cultured on the top of a coverslip slide in 6-well plates at a density of 5×10^4. HAEC cells were used as normal control cells. FITC-RRL was incubated at the concentration of 2 μg/ml after the medium was removed. After incubation for 6 h at 37 °C, the coverslips were placed on slides containing one drop of DAPI. Fluorescent images were obtained using an FV1000 confocal microscope (Olympus).

Flow Cytometry

The cellular binding of RRL to HepG2 cells was evaluated by flow cytometry. HepG2 cells were incubated with a 20 μg/ml concentration of FITC-RRL for 2 h. A control of HegG2 cells only was used. After cells were washed with cold PBS twice, they were analyzed with a BD FACSAria cytometer (Becton-Dickinson) and FlowJo analysis software (Three Star, Inc.)

Small Animal PET Imaging

HepG2 tumor-bearing mice were injected intravenously with 5.5–7.4 MBq (10 μg) of [^{68}Ga]DOTA-RRL or [^{68}Ga]$GaCl_3$ ($n = 4$). Small animal PET imaging, image reconstruction, and analysis were performed using an Inveon small animal PET scanner (Siemens Medical Solutions USA, Inc.) at 5, 15, 30, 60, and 120 min post-injection. PET images were reconstructed using a three-dimensional ordered subset expectation maximization (OSEM) algorithm. Before each PET scan, mice were anesthetized with isoflurane (2 %) and place in the scanner in a prone position. For the blocking study, mice ($n = 4$) were injected with unlabeled RRL peptide (20 mg/kg), 30 min prior to the administration of ^{68}Ga-DOTA-RRL and then scanned after 30 min.

Biodistribution Study

Following intravenous injection with 1850 kBq of [^{68}Ga]DOTA-RRL (10 μg) or [^{68}Ga]$GaCl_3$, mice were sacrificed after 5, 15, 30, 60, and 120 min, followed by collecting 100 μL of blood samples. Tissues/organs of interest (heart, liver, spleen, lung, kidney, stomach, small intestine, bladder, skeletal muscle, bone, and tumor) were harvested, weighed, and counted in a gamma counter (CNNC, China). Biodistribution results were recorded as a percentage of injected dose per gram (%ID/g). Tumor-to-nontumor (T/NT) ratios were calculated by dividing the biodistribution results of the tumor to that of the organ of interest.

Statistical Analysis

All results are expressed as the mean ± SD, and one-way ANOVA analysis was used. A confidence interval of 95 % was selected, and $P < 0.05$ was considered to be statistically significant.

Results

Radiotracer Preparation and Optimization

In order to facilitate the labeling with Ga-68, DOTA was conjugated to RRL *via* a primary amine isothiocyanate conjugation reaction (Fig. 1a). The purity of DOTA-RRL was determined using HPLC to be greater than 95 %. MALDI-TOF analysis demonstrated the molecular mass of DOTA-RRL was 1611.79, which was consistent with the calculated one (1611.87) (Fig. S1). The labeling of DOTA-RRL with Ga-68 was optimized by varying pH, temperature,

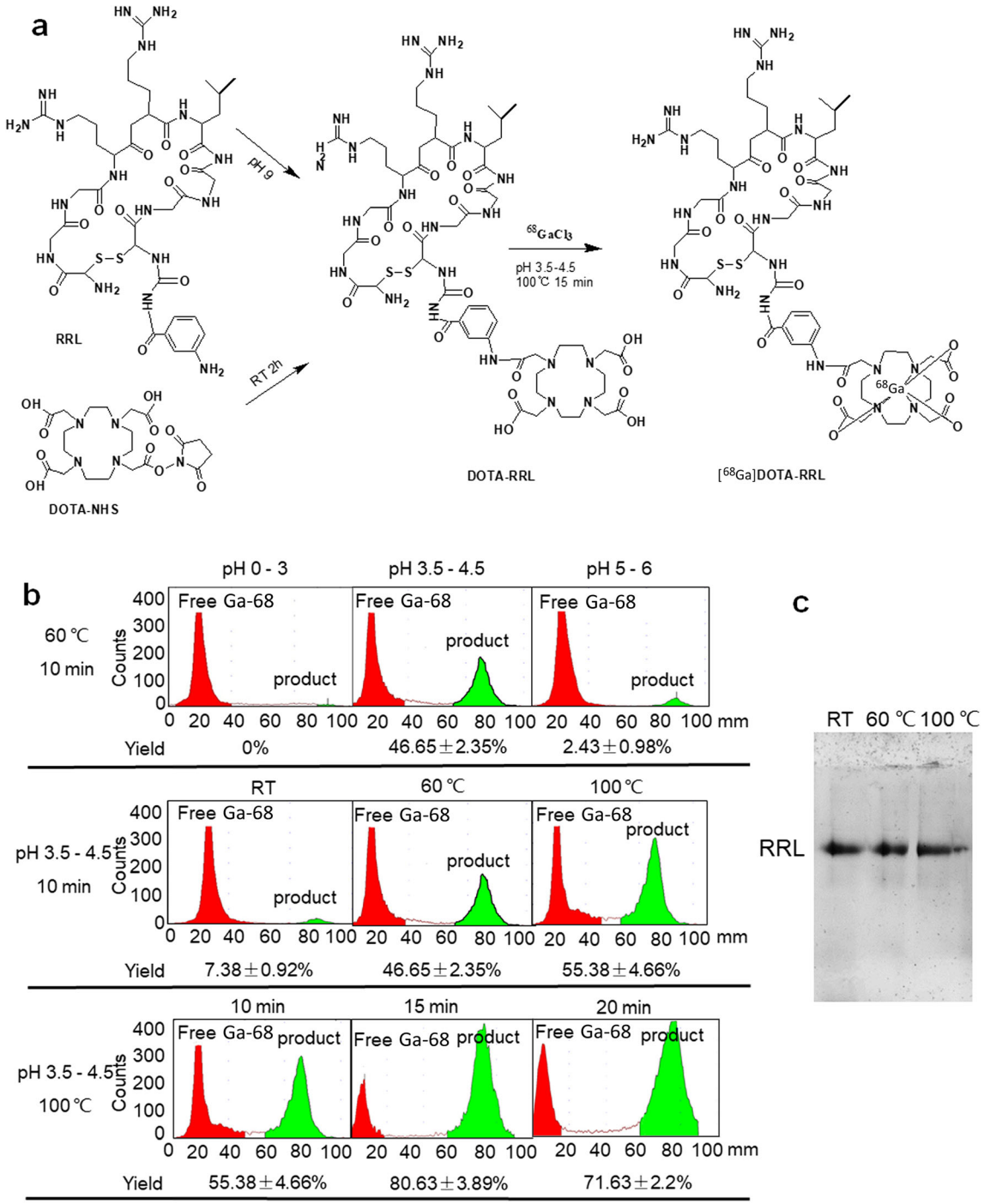

Fig. 1. Preparation and optimization of [^{68}Ga]DOTA-RRL. **a** Scheme for preparing [^{68}Ga]DOTA-RRL. RRL was conjugated with DOTA-NHS-ester and then radiolabeled with Ga-68. **b** Under different reaction conditions, the radiolabeling efficiency of [^{68}Ga]DOTA-RRL was measured to optimize the reaction. **c** SDS-PAGE analysis of DOTA-RRL after the incubation for 15 min at RT, 60 and 100 °C, respectively.

and reaction time. DOTA-RRL was successfully labeled with Ga-68 and had excellent yields (80.63 ± 3.89 %) with pH of 3.5–4.5 at 100 °C for 15 min (Fig. 1b). After purification using a PD-10 column, [^{68}Ga]DOTA-RRL had a high radiochemical purity at 97.75 ± 1.28 and specific activity at 44 GBq/μmol ($n = 5$) shown by HPLC and ITLC analysis (Fig. S2a). After incubation at RT for 2 h, [^{68}Ga]DOTA-RRL maintained the high radiochemical purity of over 95 %, shown by HPLC (Fig. S2b). Moreover, PAGE results showed that there was a single and clear band in each lane, without any degradation phenomenon, after the incubation at RT, 60 and 100 °C for 20 min (Fig. 1c).

In Vitro Stability

After incubation in fresh human serum and saline, the radiochemical purity of [^{68}Ga]DOTA-RRL was measured using ITLC. Only the radioactive peak of [^{68}Ga]DOTA-RRL was observed at each time point, while there was no obvious peak of [^{68}Ga]$GaCl_3$ (Fig. 2a). The radiolabeled product had a high radiochemical purity that was greater than 96 % (Fig. 2b) after the incubation in serum and saline. Thus, [^{68}Ga]DOTA-RRL demonstrated favorable stability in fresh human serum.

Binding Ability

The radioactive uptake of [^{68}Ga]DOTA-RRL and [^{68}Ga]$GaCl_3$ was compared after incubation with HepG2 cells. During the incubation, [^{68}Ga]DOTA-RRL showed high uptake after 30 min and reached its maximum uptake of 63.5 ± 0.64 % at 1 h. To the comparison, [^{68}Ga]$GaCl_3$ exhibited very low levels of radioactive uptake and had a maximum uptake of 1.2 ± 0.15 % at 2 h (Fig. 3a). Hence, a significant difference was found in the cellular uptake of [^{68}Ga]DOTA-RRL and [^{68}Ga]$GaCl_3$ ($t = 9.76$, $P < 0.01$). Additionally, FITC-RRL was incubated with HepG2 and HAEC cells and visualized using confocal microscopy. HepG2 cells showed enhanced cellular fluorescence while normal vessel cell line HAEC displayed weak signal (Fig. 3b). Flow cytometry results showed that FITC-RRL had high affinity with HepG2 cells, further confirming the cellular binding ability of RRL to HepG2 cells (Fig. 3c). These results indicate that RRL has a high affinity for HepG2 cells *in vitro*.

PET Imaging

PET coronal images obtained at 5, 30, 60, and 120 min post-injection are shown in Fig. 4. [^{68}Ga]DOTA-RRL and [^{68}Ga]$GaCl_3$ were injected intravenously in HepG2 tumor-bearing mice. After injection of [^{68}Ga]DOTA-RRL, PET coronal images showed clear images of HepG2 tumors. High uptake in the kidneys and bladder indicated predominant renal excretion. Tumors could be visualized clearly over time post-injection, with high tumor uptake from 30 to 60 min (Fig. 4a). To the comparison after injection of [^{68}Ga]$GaCl_3$, tumor regions showed no obvious tracer uptake. Hepatobiliary excretion was observed, which was indicated by the nonspecific uptake in the liver within 2 h (Fig. 4b). The quantitative value of tumor uptake (%ID/g) based on tumor ROI indicated that [^{68}Ga]DOTA-RRL could reach its uptake peak in tumors as quickly as 30 min post-injection (Fig. 4c).

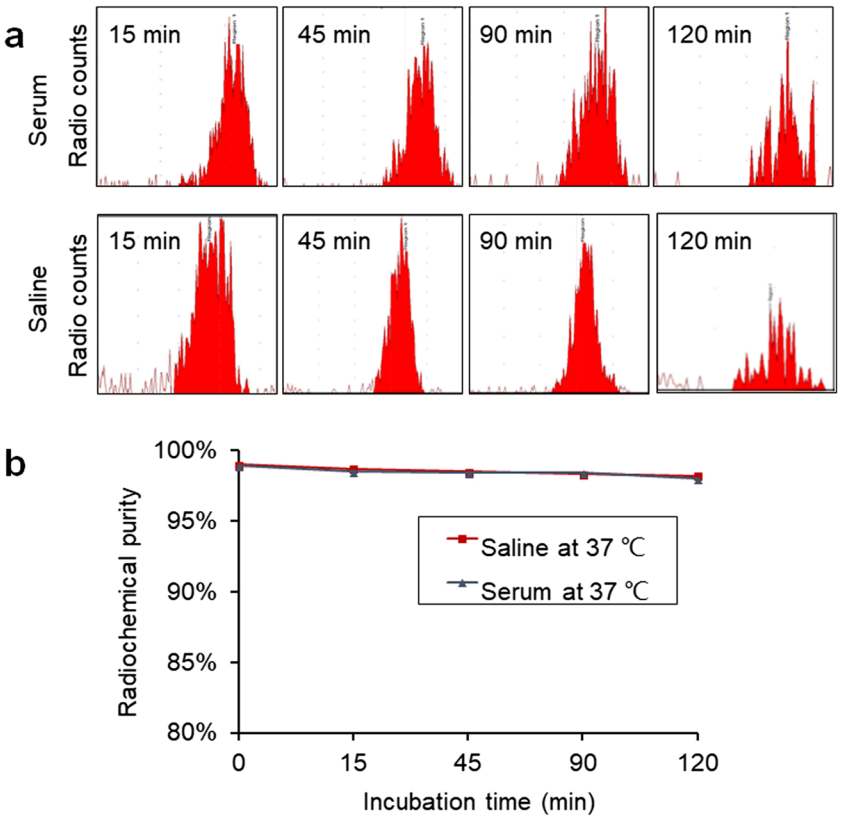

Fig. 2. Stability analysis of [^{68}Ga]DOTA-RRL in fresh human serum and saline at 15, 45, 90, and 120 min. **a** TLC and **b** radiochemical purity results.

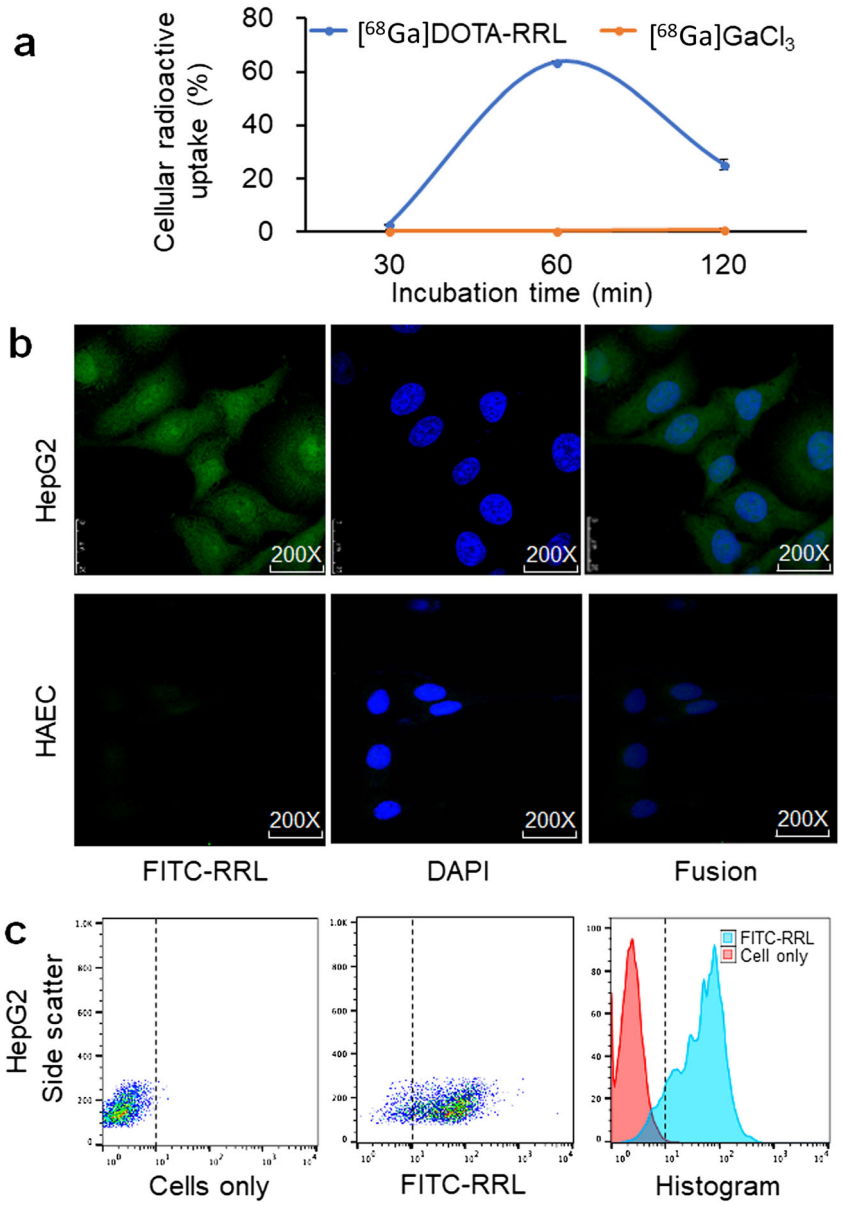

Fig. 3. Cellular binding of RRL in HepG2 cells. **a** Cellular uptake of [^{68}Ga]DOTA-RRL and [^{68}Ga]$GaCl_3$ after incubation for 120 min. Compared to [^{68}Ga]$GaCl_3$, [^{68}Ga]DOTA-RRL showed significantly higher cellular uptake after 120 min. **b** Cellular distribution of FITC-conjugated RRL in HepG2 and HAEC cells was observed using confocal microscopy. **c** FITC-conjugated RRL showed high affinity with HepG2 cells by flow cytometry.

Biodistribution

The results of biodistribution and its relevant T/NT ratios of [^{68}Ga]DOTA-RRL and [^{68}Ga]$GaCl_3$ ($n = 3$) are shown in Fig. 5 and Fig. S3, which were consistent with the PET imaging. After injection in HepG2 tumor-bearing mice, [^{68}Ga]DOTA-RRL exhibited rapid blood clearance, with 13.11 ± 0.84, 5.96 ± 0.93, and 2.19 ± 0.29 %ID/g remaining in blood at 5, 30, and 120 min, respectively. The tumor uptake of [^{68}Ga]DOTA-RRL was highest with 3.95 ± 0.71 %ID/g at 30 min and remained at 3.93 ± 0.01 %ID/g and 2.99 ± 0.21 %ID/g at 1 and 2 h post-injection, respectively. The uptake and retention of all tracers in the blood, muscle, heart, lung, liver, and bone were relatively low at 2 h post-injection. On the contrary, mice injected with [^{68}Ga]$GaCl_3$ showed very low tumor uptake of 1.35 ± 0.49, 1.22 ± 0.15, and 1.04 ± 0.16 at 5, 30, and 120 min, respectively. [^{68}Ga]$GaCl_3$ showed significantly high uptake in the spleen and liver. There were significant differences for the tumor biodistribution between [^{68}Ga]DOTA-RRL and [^{68}Ga]$GaCl_3$ group at different time points ($P < 0.05$). The T/NT ratios in muscle and blood were 11.18 ± 1.04 and 2.63 ± 0.32 after the injection of [^{68}Ga]DOTA-RRL, while those were 3.71 ± 0.56 and 0.29 ± 0.01 after the injection of [^{68}Ga]$GaCl_3$.

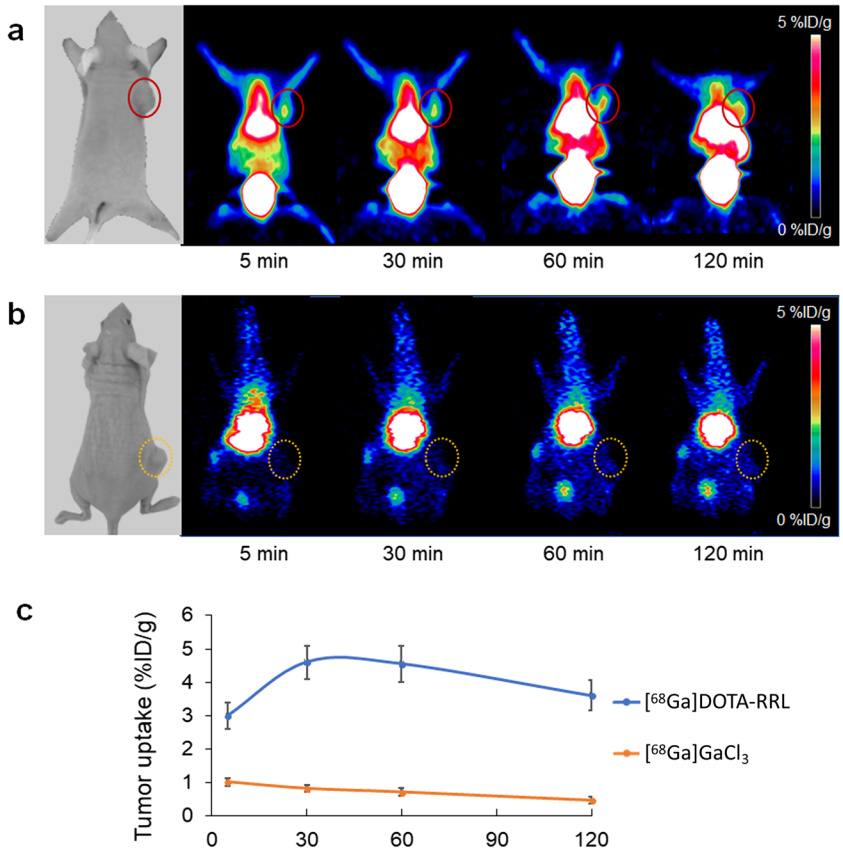

Fig. 4. PET coronal images of HepG2 tumor-bearing mice after injection of **a** [^{68}Ga]DOTA-RRL or **b** [^{68}Ga]$GaCl_3$ (b) at 5, 30, 60, and 120 min, respectively (circles indicate tumor region), as well as **c** the quantitative value of tumor uptake by drawing ROI. The tumor showed high radioactive uptake from 5 to 120 min post-injection of [^{68}Ga]DOTA-RRL, while [^{68}Ga]$GaCl_3$ did not visualize the tumor.

Blocking Study

In the blocking study, PET imaging and biodistribution analysis were performed in HepG2 tumor-bearing mice ($n = 3$) pre-injected with cold RRL at 30 min prior to injection of [^{68}Ga]DOTA-RRL. After pre-treatment of cold RRL, tumor region could not be visualized clearly in maximum-intensity projection (MIP), coronal and axial images (Fig. 6a), suggesting uptake of [^{68}Ga]DOTA-RRL in the tumor was competed by cold RRL. Moreover, biodistribution results showed the tumor uptake was only 1.28 ± 0.04 %ID/g after blocking, while the tumor uptake was 3.95 ± 0.71 %ID/g without blocking ($P < 0.05$). Compared with unblocked mice, increased uptakes were observed for the blocked mice in the heart, spleen, lung, stomach, and small intestine, but decreased in the tumor ($P < 0.05$). T/NT ratios of muscle and blood were 1.00 ± 0.49 and 0.23 ± 0.12 after cold RRL blocking, which was significantly decreased after injection of [^{68}Ga]DOTA-RRL ($P < 0.01$) (Fig. 6b).

Discussion

Small molecule peptides have been used widely in tumor diagnosis because of their excellent biological properties. First, their low molecular weight induces no immunogenicity and reduces the nonspecific uptake by the reticular endothelial system in the liver [1]. Second, compared with whole antibodies, small molecule peptides are more stable in biological systems with high affinities and specificities for their receptors. Finally, small molecule compounds can be easily modified to improve *in vivo* performance [21].

In this study, we designed a RRL-contained peptide and radiolabeled the peptide with Ga-68 *via* the conjugation of DOTA to develop a novel PET tumor imaging probe. Under optimized conditions, [^{68}Ga]DOTA-RRL had a high labeling yield and favorable human serum stability. RRL showed high cellular radioactive uptake and fluorescent binding in HepG2 cell line. Clear tumor uptake was noted in HepG2 xenografts at 30 min post-injection of [^{68}Ga]DOTA-RRL. Moreover, significantly higher tumor uptake levels of [^{68}Ga]DOTA-RRL were observed than those after the blocking with cold RRL in PET imaging and biodistribution studies. These results support the potential of [^{68}Ga]DOTA-RRL as a tumor imaging probe for future applications.

The RRL peptide was initially developed as a vascular endothelial cell-specific binding small molecule [2] and later

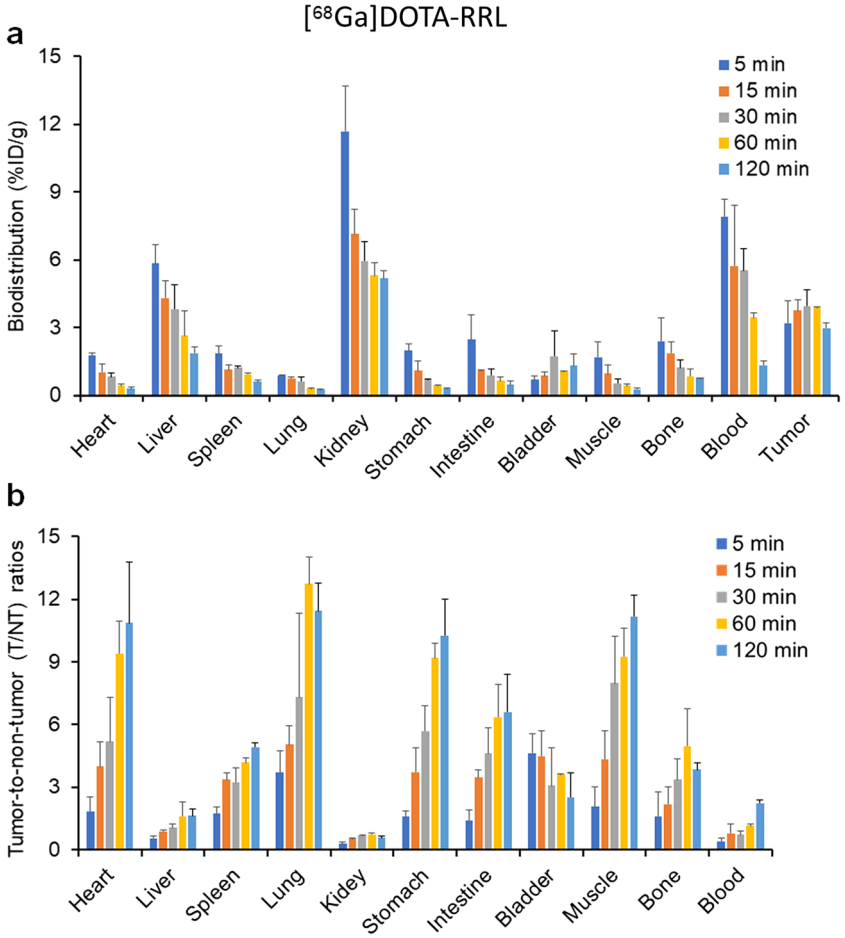

Fig. 5. **a** Biodistribution and **b** its related tumor-to-nontumor (T/NT) ratios of [^{68}Ga]DOTA-RRL in HepG2 tumor-bearing mice over 2 h post-injection.

extended to bind to tumor cells as well [6, 11]. In our previous studies, RRL was found to target tumor vascular endothelial cells as well as tumor parenchyma in [^{131}I]RRL and FITC-RRL binding studies [3]. RRL has been successfully radiolabeled with single photon emission isotopes, such as I-131 and Tc-99m, in the SPECT imaging of prostate cancer, melanoma, liver cancer, lung metastases, and angiosarcoma tumor models [6, 8–11]. A Tc-99m-labeled hexapeptide RRL peptide also demonstrated increased uptake in fibrosarcoma tumors compared with inflammation lesion [7]. However, there have been no previous studies on a radiolabeled RRL-related peptide with positron emitting isotopes for PET imaging. This study firstly employs a Ga-68-labeled RRL peptide for PET imaging in hepatocellular carcinoma. PET imaging was utilized because it provides better resolution and sensitivity. Tumor accumulation of [^{68}Ga]DOTA-RRL reached a maximum at 30 min and remained high at 60 min post-injection, which was quicker than that of Tc-99m- and I-131-labeled RRL in our previous imaging studies (6 and 24 h respectively) [8–11]. The decreased time between injection and imaging provides better availability for tumor imaging and potential usage in the clinic because patients do not need to wait for a long time for imaging post-injection.

As a small molecular weight peptide, RRL might pass through the membrane of tumor cells *via* passive effect or some possible targeted receptor, such as VEGFR [3, 6]. The cellular uptake reached its peak at 60 min but decreased in 120 min, which might be caused by passive effusion from cancer cells. After diffused into the cytoplasm, RRL could further bind to some nucleosomes in nuclei, shown by FITC-RRL uptake *in vitro*. After intravenous injection, it showed uptake peak at 30 min and remained high at 60 min post-injection (3.95 ± 0.71 %ID/g and 3.93 ± 0.01 %ID/g) and decreased after 120 min (2.99 ± 0.21 %ID/g). Although the washout of RRL probe was also observed *in vivo* study, it was slower than that in tumor cellular uptake, which might be affected by complex factors *in vivo*. The possible mechanism of [^{68}Ga]DOTA-RRL *in vivo* might be related with tumor EPR effect, internalization *via* some targeted receptors expressed in different membrane structure, or some specific ligands expressed in tumor-derived endothelial cells (TDECs), mentioned in our previous study [6]. Compared with other RRL probes, [^{68}Ga]DOTA-RRL shows better

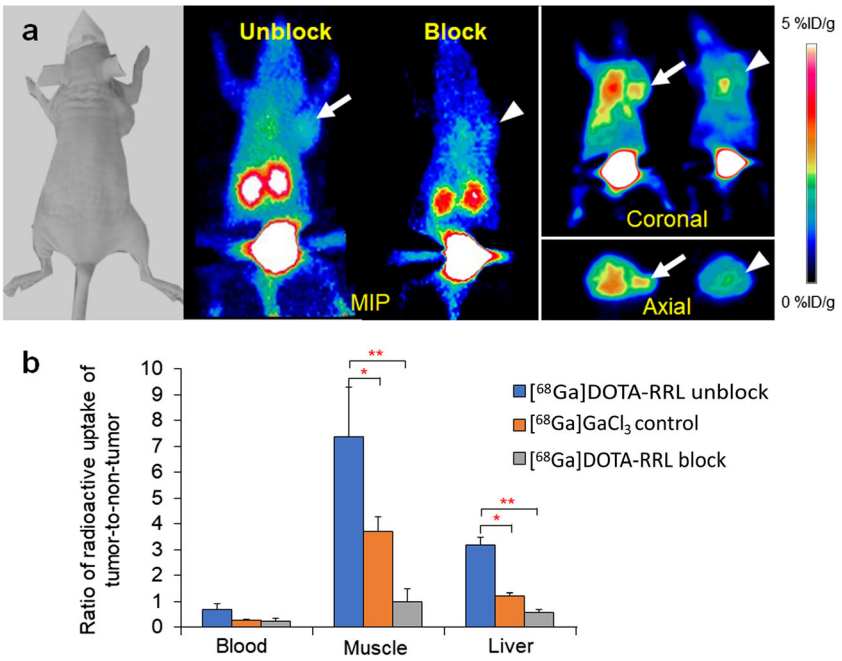

Fig. 6. Blocking study. **a** MIP, coronal, and axial PET images and **b** T/NT ratios in HepG2 tumor-bearing mice with pre-injection of cold RRL (short arrow) or not (long arrow) at 30 min after injection of [^{68}Ga]DOTA-RRL (arrows indicate tumor region). The tumor could not be seen after blocking with cold RRL. T/NT ratios in muscle and liver were higher than those after blocking (** means $P < 0.01$, * means $P < 0.05$).

resolution and higher contrast in PET imaging and should retain similar tumor uptake mechanism. However, the precise mechanisms still need to be further investigated.

The sequence of RRL peptide in this study is different from our previous studies. In this study, triple peptides Cys-Gly-Gly and 4-Abz were used to improve the stability and binding affinity. Biodistribution results revealed that higher tumor uptake was obtained after this chemical modification. For the same liver cancer model (HepG2 model), tumor uptake reached 2.1 ± 0.3 %ID/g in this study which was higher than [^{131}I]RRL (1.5 %ID/g) or [^{99m}Tc]RRL (from 3.17 ± 0.63 to 5.25 ± 1.52 %ID/g) [10]. In this study, the ratios of the tumor-to-muscle exceeded 11.2, tumor-to-liver reached 1.62, and tumor-to-blood reached 2.23, higher than those from [^{99m}Tc]RRL. The liver uptake was low after the injection of [^{68}Ga]DOTA-RRL, with a tumor-to-liver ratio of 3.54 ± 0.58 at 2 h. The biodistribution results in blood at 30 min (5.96 ± 0.93 %ID/g) and at 2 h (2.19 ± 0.29 %ID/g at 2 h) indicate decreased background and better contrast for ^{68}Ga-DOTA-RRL in PET imaging. Therefore, [^{68}Ga]DOTA-RRL showed good tumor binding ability.

For developing Ga-68-labeled probes, bifunctional chelating is one of the most common methods [16, 22]. Macrocyclic DOTA and NOTA derivative conjugators have open chains that are easily conjugated [22]. DOTA derivative (DOTA-NHS) is a tetraazacycle bifunctional chelator that can select three carboxyl groups for protection, functionalization, and deprotection and ensures that only one carboxyl group participates in cross-linking reaction [23]. This provides a mild condition for labeling proteins or peptides with a slow rate of hydrolysis [24]. Since DOTA derivatives have good thermodynamic stability and kinetic properties, the ^{68}Ga labeling yields and tumor uptake rates are relatively high [25]. However, [^{68}Ga]$GaCl_3$ is readily hydrolyzed to form $Ga(OH)_3$ colloids when pH is greater than 5, which decreases the radiolabeling efficiency [26]. In our study, acidic pH also favored the protonation of four carboxyl groups on DOTA and increased the labeling efficiency. The highest radiolabeling efficiency was obtained with a pH between 3.5 and 4.5. The labeling yield was significantly higher than that of [^{99m}Tc]RRL (76.9 ± 4.5 %) and [^{131}I]RRL (70.0 ± 2.9 %) in our previous studies [9, 10]. Besides, reaction temperature affects the labeling efficiency. In a previous study, DOTA-somatostatin analogs were radiolabeled with In-111, Y-90 or Lu-177 at 95 °C for 25 min or 80 °C for 20 min, resulting in nearly 100 % labeling yield [27]. In this study, the optimized labeling yield was acquired when the reaction was performed at 100 °C for 15 min. This high radiolabeling efficiency provided the better need for animal imaging.

The RRL peptide showed high radioactive cellular uptake and fluorescent affinity using confocal microscopy and flow cytometry. After incubation at 100 °C for 20 min, RRL showed a clear and integrated band by SDS-PAGE gel analysis. Compared to [^{68}Ga]$GaCl_3$, [^{68}Ga]DOTA-RRL was able to visualize the tumor images. Moreover, the tumor-

specificity of [^{68}Ga]DOTA-RRL probe was also illustrated with block imaging results. Tumor images were not visualized by [^{68}Ga]DOTA-RRL after the blocking with cold RRL, indicating that unlabeled RRL competed to bind to the HepG2 tumor with [^{68}Ga]DOTA-RRL. So far, RRL relative radiolabeled probes have been used in several malignant tumors such as prostate carcinoma [24], melanoma [27], lung metastasis [12], and liver cancer [26]. Based on the previous study, RRL-related probes could mainly target TDECs and become a candidate imaging agent for tumor angiogenesis. For those tumors rich in tumor angiogenesis and relative ligands highly expressed in TDECs, RRL probes could be used for imaging. Besides, as a potential imaging agent, cytotoxicity is always a key fact. RRL was not toxic to vascular endothelial cells, normal cells, and tumor cells [10]. Therefore, radiolabeled RRL showed highly safe, targeted tumor neonatal small molecule peptide probe [12].

Conclusions

In this study, Ga-68-labeled RRL was prepared with a high labeling yield and stability *via* the conjugation of DOTA. [^{68}Ga]DOTA-RRL showed a high affinity to hepatocarcinoma cells and had a high and specific tumor uptake in tumor xenografts. Therefore, [^{68}Ga]DOTA-RRL provides a novel noninvasive and efficient PET imaging agent for tumor diagnosis.

Funding Information. This study was supported by grants from the National Special Fund for the Development of Major Research Equipment and Instruments (2011YQ03011409), Twelfth "Five-Year" Plan for Science & Technology Support (2014BAA03B03), Beijing Nova Program (Z171100001117024, Z181100006218126), Beijing Capital Special Development Application Program (Z141107002514159) and Peking University First Hospital Youth Program (2017QN13, 2017QN14).

Compliance with Ethical Standards

Conflict of Interest

The authors declare that they have no conflict of interest.

Ethical Approval

All applicable international, national, and/or institutional guidelines for the care and use of animals were followed.

References

1. Sun X, Li Y, Liu T et al (2016) Peptide-based imaging agents for cancer detection. Adv Drug Deliv Rev 110-111:38–51
2. Brown CK, Modzelewski RA, Johnson CS, Wong MK (2000) A novel approach for the identification of unique tumor vasculature binding peptides using an E. coli peptide display library. Ann Surg Oncol 7:743–749
3. Lu X, Wang RF (2012) A concise review of current radiopharmaceuticals in tumor angiogenesis imaging. Curr Pharm Des 18:1032–1040
4. Weller GE, Wong MK, Modzelewski RA, Lu E, Klibanov AL, Wagner WR, Villanueva FS (2005) Ultrasonic imaging of tumor angiogenesis using contrast microbubbles targeted via the tumor-binding peptide arginine-arginine-leucine. Cancer Res 65:533–539
5. Weller GE, Villanueva FS, Klibanov AL, Wagner WR (2002) Modulating targeted adhesion of an ultrasound contrast agent to dysfunctional endothelium. Ann Biomed Eng 30:1012–1019
6. Lu X, Yan P, Wang RF, Liu M, Yu MM, Zhang CL (2012) Use of radioiodinated peptide Arg-Arg-Leu targeted to neovascularization as well as tumor cells in molecular tumor imaging. Chinese J Cancer Res 24:52–59
7. Kim DW, Kim WH, Kim MH, Kim CG (2015) Synthesis and evaluation of Tc-99m-labeled RRL-containing peptide as a non-invasive tumor imaging agent in a mouse fibrosarcoma model. Ann Nucl Med 29:779–785
8. Yu M, Zhou H, Liu X et al (2010) Study on biodistribution and imaging of radioiodinated arginine-arginine-leucine peptide in nude mice bearing human prostate carcinoma. Ann Nucl Med 24:13–19
9. Zhao Q, Yan P, Yin L et al (2013) Validation study of (1)(3)(1)I-RRL: assessment of biodistribution, SPECT imaging and radiation dosimetry in mice. Mol Med Rep 7:1355–1360
10. Zhao Q, Yan P, Wang RF et al (2013) A novel ^{99m}Tc-labeled molecular probe for tumor angiogenesis imaging in hepatoma xenografts model: a pilot study. PLoS One 8:e61043
11. Lu X, Zhao L, Xue T, Zhang H (2013) Technetium-99m-Arg-Arg-Leu(g2), a modified peptide probe targeted to neovascularization in molecular tumor imaging. J BUON 18:1074–1081
12. Yao N, Yan P, Wang RF, Zhang CL, Ma C, Chen XQ, Zhao Q, Hao P (2015) Detection of pulmonary metastases with the novel radiolabeled molecular probe, ^{99m}Tc-RRL. Int J Clin Exp Med 8:1726–1736
13. Kang L, Wang RF, Yan P, Liu M, Zhang CL, Yu MM, Cui YG, Xu XJ (2010) Noninvasive visualization of RNA delivery with 99mTc-radiolabeled small-interference RNA in tumor xenografts. J Nucl Med 51:978–986
14. Lang L, Li W, Guo N, Ma Y, Zhu L, Kiesewetter DO, Shen B, Niu G, Chen X (2011) Comparison study of [^{18}F]FAl-NOTA-PRGD2, [18F]FPPRGD2, and [^{68}Ga]Ga-NOTA-PRGD2 for PET imaging of U87MG tumors in mice. Bioconjug Chem 22:2415–2422
15. Oxboel J, Brandt-Larsen M, Schjoeth-Eskesen C, Myschetzky R, el-Ali HH, Madsen J, Kjaer A (2014) Comparison of two new angiogenesis PET tracers ^{68}Ga-NODAGA-E[c(RGDyK)]2 and ^{64}Cu-NODAGA-E[c(RGDyK)]2; in vivo imaging studies in human xenograft tumors. Nucl Med Biol 41:259–267
16. Notni J, Pohle K, Wester HJ (2012) Comparative gallium-68 labeling of TRAP-, NOTA-, and DOTA-peptides: practical consequences for the future of gallium-68-PET. EJNMMI Res 2:28
17. Shan L (2004) ^{131}I-Labeled arginine-arginine-leucine (RRL)-containing cyclic peptide (YCGGRRLGGC) for imaging prostate carcinoma. In: Molecular Imaging and Contrast Agent Database (MICAD). Bethesda (MD)
18. Geng H, Jiang F, Wu YD (2016) Accurate structure prediction and conformational analysis of cyclic peptides with residue-specific force fields. J Phys Chem Lett 7:1805–1810
19. Price EW, Orvig C (2014) Matching chelators to radiometals for radiopharmaceuticals. Chem Soc Rev 43:260–290
20. Poschenrieder A, Schottelius M, Schwaiger M, Wester HJ (2016) Preclinical evaluation of [^{68}Ga]NOTA-pentixafor for PET imaging of CXCR4 expression in vivo—a comparison to [^{68}Ga]pentixafor. EJNMMI Res 6:70
21. Zhao N, Qin Y, Liu H, Cheng Z (2018) Tumor-targeting peptides: ligands for molecular imaging and therapy. Anti Cancer Agents Med Chem 18:74–86
22. Romero E, Martinez A, Oteo M et al (2016) Preparation of ^{68}Ga-labelled DOTA-peptides using a manual labelling approach for small-animal PET imaging. Appl Radiat Isot 107:113–120
23. Tolmachev V, Velikyan I, Sandstrom M, Orlova A (2010) A HER2-binding Affibody molecule labelled with ^{68}Ga for PET imaging: direct in vivo comparison with the 111In-labelled analogue. Eur J Nucl Med Mol Imaging 37:1356–1367
24. Mohsin H, Fitzsimmons J, Shelton T, Hoffman TJ, Cutler CS, Lewis MR, Athey PS, Gulyas G, Kiefer GE, Frank RK, Simon J, Lever SZ, Jurisson SS (2007) Preparation and biological evaluation of ^{111}In-,

^{177}Lu- and ^{90}Y-labeled DOTA analogues conjugated to B72.3. Nucl Med Biol 34:493–502
25. Antunes P, Ginj M, Zhang H, Waser B, Baum RP, Reubi JC, Maecke H (2007) Are radiogallium-labelled DOTA-conjugated somatostatin analogues superior to those labelled with other radiometals? Eur J Nucl Med Mol Imaging 34:982–993
26. Jackson GE, Byrne MJ (1996) Metal ion speciation in blood plasma: gallium-67-citrate and MRI contrast agents. J Nucl Med 37:379–386
27. Fortin MA, Orlova A, Malmstrom PU, Tolmachev V (2007) Labelling chemistry and characterization of [^{90}Y/^{177}Lu]-DOTA-ZHER2:342-3 Affibody molecule, a candidate agent for locoregional treatment of urinary bladder carcinoma. Int J Mol Med 19:285–291